ATTENUATION MEASUREMENT

When a signal is sent along any transmission path, many different mechanisms degrade it. Because of finite conductivity, every cable shows a resistive loss. Furthermore, the dielectric loss and the skin effect may be significant at higher frequencies, and imperfect screening of cables leads to radiation losses which might be quite important at higher frequencies. Single-mode optical fibers have two main intrinsic loss mechanisms, scattering loss and absorption loss. Scattering loss is dominated by Rayleigh scattering, and below 1600 nm absorption losses are caused mainly by OH absorption. Fibers that are bent too tightly or cabled too poorly may have, in addition, bend losses because of nonguided modes. Connectors show losses because of nonideal contacts and imperfect impedance matching, which reflect part of the signal to the transmitter. Filters built in the transmission path have losses in the passband caused by finite conductivity and probably dielectric losses. Wireless transmission paths, such as microwave links, satellite links, broadcast or mobile communication, are affected by scattering caused by rain, clouds, and multiple reflections.

The two examples following clearly show how additional attenuation or losses influence a system:

> In a radar system a total loss of 2 dB in the feeder system and the duplexer wastes 37% of the transmitter power. During the development of the different parts, the losses have to be measured very carefully to minimize the total loss.
>
> Satellite systems quite often operate with cooled front ends at the receiver because the signals to be picked up are extremely weak. Therefore the front ends often operate with noise temperatures of 5 K. An additional loss of 0.1 dB from an uncooled waveguide would raise the noise temperature to 7 K.

These examples show how important it is to measure the losses of the different parts of a transmission system as accurately as possible to optimize system parameters.

Many different methods and a variety of systems for measuring attenuation have been developed. The most important techniques are described in the following sections.

ATTENUATION

Definition

In the field of loss measurement, the most important terms are attenuation, insertion loss, mismatch loss and voltage loss (1,2). These terms are discussed in the following sections.

Attenuation. According to R. W. Beatty (3), attenuation is defined as the decrease in power level at the load caused by inserting a device between a Z_0 source and load, where Z_0 is the characteristic impedance of the line. Figure 1 shows the basic idea of such an attenuation measurement.

Attenuation is mostly expressed by a logarithmic scale in decibels (dB) or in nepers. The attenuation of a two-port device is defined as follows (4):

in decibels,

$$A = 10\log\left[\frac{\text{power delivered to a matched load by a matched source}}{\text{power delivered to the same load when the two-port device is inserted}}\right] \tag{1}$$

in nepers,

$$A = \tfrac{1}{2}\ln\left[\frac{\text{power delivered to a matched load by a matched source}}{\text{power delivered to the same load when the two-port device is inserted}}\right] \tag{2}$$

Because $\log(x) = \ln(x)/\ln(10)$, the following relationship between decibels and nepers is valid:

$$\text{Attenuation in decibels} = 8.6858 \times \text{attenuation in nepers}$$

Attenuation is a property only of a two-port device.

Insertion Loss. In practical applications neither the source nor the load have an impedance exactly equal to Z_0 the characteristic impedance of a line. Therefore source and load have a reflection coefficient of r_s and r_L, respectively. Let P_1 be the power delivered from the source to the load and P_2 be the power absorbed by the same load when the two-port device is inserted (Fig. 2.)

Then the loss is defined by

$$L_1 = 10\log\frac{P_1}{P_2} \tag{3}$$

The insertion loss depends on the property of the device and the reflection coefficients of the source and the load.

Scattering Parameters. Two-port networks, especially at radio frequencies, are very well characterized by scattering parameters.

A two-port device inserted between a source and a load is shown in Fig. 3.

The complex wave amplitudes a_1, a_2, b_1, and b_2 shown in Fig. 3 are related as follows:

$$b_1 = s_{11}a_1 + s_{12}a_2 \tag{4}$$

and

$$b_2 = s_{21}a_1 + s_{22}a_2 \tag{5}$$

Setting up the signal flow graph for the configuration in Fig. 3 and using the nontouching loop rules of Mason (5,6), the insertion loss is given by the following expression:

$$L_I = 20\log\frac{|(1 - r_s s_{11})(1 - r_L s_{22}) - r_s r_L s_{12}s_{21}|}{|s_{21}|\cdot|1 - r_s r_L|} \tag{6}$$

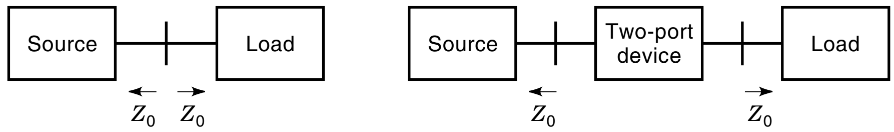

Figure 1. Attenuation measurement in a matched system.

For a matched system where $r_s = r_L = 0$, Eq. (6) delivers the attenuation

$$A = 20 \log \frac{1}{|s_{21}|} \tag{7}$$

Equations (6) and (7) clearly show that the insertion loss L_I depends on the property of the two-port device and the reflection coefficients of the source r_s and the load r_L. Otherwise the attenuation is the pure property of the two-port device.

Voltage Loss. Voltage loss is used only for applications in the dc to UHF part of the spectrum where voltage is well defined. According to Warner (4), it is defined as follows:

$$L_V = 20 \log \left[\frac{\text{voltage at the input of the two-port device}}{\text{voltage at the output of the two-port device}} \right] \tag{8}$$

and using the scattering parameters

$$L_V = 20 \log \frac{|(1 + s_{11})(1 - r_L s_{22}) + r_L s_{12} s_{21}|}{|s_{21}(1 - r_L)|} \tag{9}$$

Note that L_V is independent of the source reflection coefficient r_s.

When $s_{11} = 0$ and $r_L = 0$, the voltage loss is equal to the attenuation.

Mismatch Loss. At higher frequencies every real two-port device has an input and output reflection coefficient that differs from zero. Therefore, there is always a mismatch between the source and the two-port device and between the two-port device and the load (Fig. 4). This reflects part of the incoming and outgoing wave toward the source and toward the two-port device, respectively, resulting in additional losses.

The mismatch loss between the source and the two-port device is expressed as:

$$L_{m1} = 10 \log \frac{\text{power absorbed at the input of the two-port device}}{\text{maximal available power from the source}} \tag{10}$$

According to Fig. 3 the mismatch loss is given by

$$L_{m1} = \frac{(1 - |r_s|^2)(1 - |r_1|^2)}{|1 - r_s r_1|^2} \tag{11}$$

Similarly, the mismatch loss between the two-port device and the load is given by

$$L_{m2} = 10 \log \frac{\text{power absorbed by the load}}{\text{maximal available power at the output of the two-port device}} \tag{12}$$

and with the parameters of Fig. 4

$$L_{m2} = 10 \log \frac{(1 - |r_2|^2)(1 - |r_L|^2)}{|1 - r_2 r_L|^2} \tag{13}$$

If several two-port devices are cascaded, the mismatch loss between them has to be calculated similarly and taken into account.

ATTENUATOR

Apart from the natural losses in devices and transmission paths, manufactured devices have well-defined losses. These devices called attenuators are used for measurement and for adjusting power levels to a defined value in transmission systems. Attenuators are probably the most important devices in measurement systems and therefore exist in a large number of different forms (7–9), such as symmetrical, coaxial, waveguide, optical, fixed-value, and variable-loss. The important properties of attenuators are: frequency range, attenuation accuracy, attenuation variation versus frequency, input and output impedance match (reflection coefficient), power handling capacity, and phase linearity.

Balanced-Line Attenuator

Balanced lines are used especially in telecommunications and lately in local area networks and in-house communications systems. Therefore, there is a demand for balanced-line attenuators. Chains of symmetrical double-T or double-Π circuits, as shown in Fig. 5, are mostly used (10).

The reference handbooks (10) give formulas and tables to determine the circuit elements for a given line impedance and different element attenuations. The circuit has to be symmetrical to the ground plane and well matched to the line impedance. Special techniques are given to optimize the circuit for small frequency dependency.

Variable-value attenuators are commercially available for different impedances (150 Ω, 120 Ω) in the frequency range

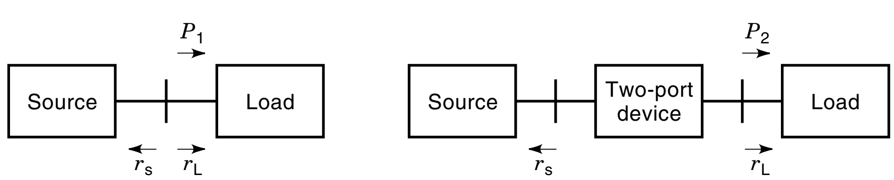

Figure 2. Insertion loss measurement in a nonmatched system.

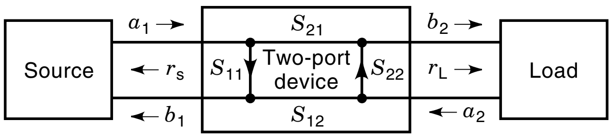

Figure 3. Scattering parameters for a two-port device inserted between source and load.

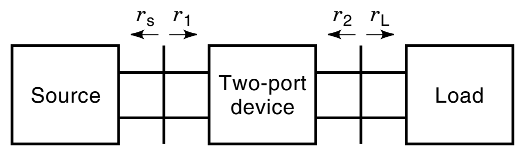

Figure 4. Mismatch loss of a two-port device between a source and a load.

from dc to several megahertz and have attenuation ranges from 0 dB to 132 dB.

Coaxial-Line Attenuator

Fixed-Value Coaxial Attenuator. Coaxial attenuators generally have multioctave bandwidth or frequently operate from dc to several gigahertz (GHz). Coaxial transmission lines are generally operated in the transverse electromagnetic (TEM) mode and therefore an obvious solution for attenuators is to use lumped elements that are small compared to the wavelength. There are four major constructions: T-circuit, Π-circuit, distributed lossy line and distributed thin-film technology.

T-Circuit Attenuator. The T-attenuator circuit is shown in Fig. 6. The values of R_1 and R_2 are calculated from the following formulas, where K is the transmission coefficient (7,10).

$$R_1 = Z_0 \frac{K-1}{K+1} \tag{14}$$

$$R_2 = \frac{2Z_0K}{K^2-1} \tag{15}$$

The attenuation in decibels is given by

$$A(\mathrm{dB}) = 20 \log K \tag{16}$$

Resistive rods for R_1 are often used, and disk resistors are used for R_2, or film resistors are used for both R_1 and R_2.

Π-Circuit Attenuator. Techniques similar to the T-circuit are used for the Π-circuit shown in Fig. 7, and the corresponding formulas are as follows (7,10):

$$R_1 = Z_0 \frac{K+1}{K-1} \tag{17}$$

$$R_2 = Z_0 \frac{K^2-1}{2K} \tag{18}$$

At higher microwave frequencies the elements of the T- and Π-attenuators have dimensions comparable to the wavelength, and therefore the reactance of the elements gets more important and therefore degrades the performance of the attenuator.

Lossy-Line Attenuator. Distributed lossy-line attenuators, explained by Weber (11), have very favorable performance. As long as the attenuation is not very high, they have a flat attenuation response and an excellent impedance match. The center conductor of the transmission line is mostly made of lossy material using thin film deposited on a substrate with a circular cross section. The disadvantage of lossy-line attenuators is that they have a lower frequency limit depending on their physical length.

Thin-Film Attenuator. Distributed thin-film attenuators (12) use a resistive material deposited on a dielectric substrate for the series and shunt losses (Fig. 8).

Strip transmission lines and narrow ground electrodes on the longitudinal sides are added to the input and output terminals. The characteristic impedance and the attenuation are constant and given as follows (7):

TART Numbered Equation 19

$$Z_0 = \rho \sqrt{\frac{D-a}{4a}} \qquad (\Omega) \tag{19}$$

$$\alpha = \sqrt{\frac{4}{a(D-a)}} \qquad \text{(in nepers per unit length)} \tag{20}$$

Equation 20 shows that the attenuation is independent of the resistivity of the film as long as the film is homogenous. The attenuation depends only on the geometry and therefore is insensitive to temperature changes.

Variable-Value Coaxial Attenuator. There are two types of variable attenuators: continuous variable attenuators and step attenuators. Continuous variable attenuators have the advantage of being noninterruptive when changing attenuation. This feature is important for some measurements, for example, receiver sensitivity measurements. On the other hand, these attenuators may sometimes lack accuracy, setta-

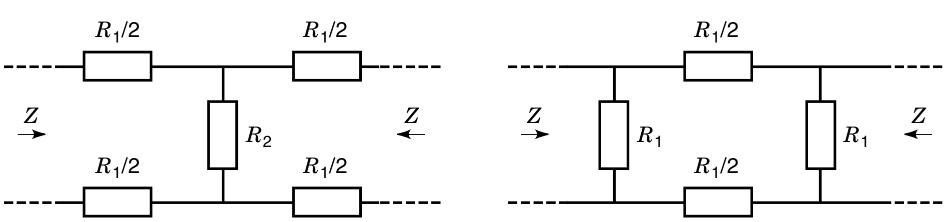

Figure 5. Basic symmetrical double-T and double-Π attenuation circuits.

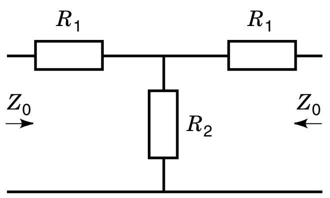

Figure 6. T-attenuator circuit.

bility, impedance match, high insertion loss and have limited bandwidth.

Step attenuators are very accurate and have the following qualities: good reproduceability, low insertion loss, excellent impedance match, and wide operating bandwidth. But most step attenuators are interruptive when changing the attenuation value.

Continuously Variable Attenuator

Piston Attenuator (Waveguide Beyond Cutoff Attenuator). The piston attenuator is one of the oldest continuously variable microwave attenuators (13). It is used especially as a precision attenuator or for handling high power levels. This type of attenuator uses a waveguide below its cutoff frequency. According to transmission line theory, the amplitude of a wave launched into such a waveguide decays exponentially. So the attenuation is calculable. Most constructions use a circular cross section and a magnetic coupling that generates the lowest cutoff higher order transverse electric mode (TE_{11}). Figure 9 shows the simplified construction of a piston attenuator. By sliding the two concentric cylinders into each other, the physical displacement of the coupling coil is changed and therefore also the attenuation. Special care must be taken to avoid unwanted higher order modes.

Attenuation as a function of wavelength is given per unit length as (10)

$$A = \frac{2\pi \cdot 20}{\lambda_c \cdot \ln 10}\sqrt{1-\left(\frac{\lambda_c}{\lambda}\right)^2} \qquad \text{in decibels per unit length} \quad (21)$$

where λ_c is the cutoff wavelength of the waveguide and λ is the free-space wavelength.

If the operating frequency is chosen to be much lower than the cutoff frequency, the term λ_c/λ is negligibly small for the operating frequency band, and a flat attenuation frequency response is achieved. The advantages of cutoff attenuators are that they are calculable and that high accuracy is achieved (0.001 dB/10 dB for 60 dB attenuation). For this reason, cutoff attenuators are often used as standard attenuators. Their main disadvantage is the high insertion loss (15 to 20 dB) because tight coupling has to be avoided so as not to stimulate higher modes.

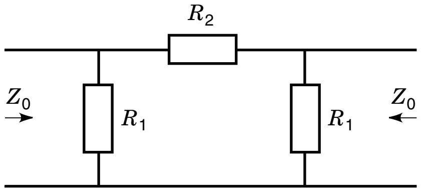

Figure 7. Π-attenuator circuit.

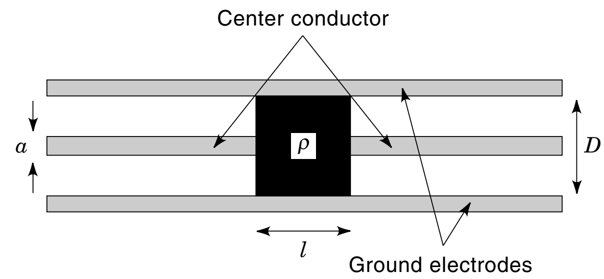

Figure 8. Distributed thin-film attenuator element.

Resistant Card, T-, or Π*-Type Attenuator.* Several constructions of variable attenuators using resistive cards or resistive films are on the market (9). The variable card attenuator operates like a potentiometer. A resistive film is fixed on a substrate so that the resistance between the input and the output is varied with a movable coaxial wiper, and thus the amount of attenuation changes. This type of attenuator does not have good input and output impedance matches. More sophisticated constructions use T- or Π-type structures where the series and the shunt resistors are changed simultaneously. Therefore the input and output ports of these attenuators are quite well matched. The minimum insertion loss is on the order of 4 dB, and they operate up to several gigahertz.

Lossy-Line Attenuator. Lossy-line attenuators use a lossy center conductor partly covered with a thin sliding shield (7). This effectively changes the length of the resistive conductor and thus the attenuation. Some constructions use microstrip lines with variable lossy walls (9). This type of attenuator is limited in its maximal attenuation because of the length of the device.

Pin Attenuator. *Pin* attenuators change the loss in either a step or continuous mode. The series and shunt resistors are replaced by *pin* diodes, electronic devices that change their conductivity. The diodes are controlled by a bias current. Various types of circuits are available, such as series, shunt, bridged T, and Π (9). *Pin* attenuators are electronic circuits and therefore may produce harmonics. Below about 10 MHz, the *pin* diode exhibits some rectifying behavior. At much higher frequencies, the *pin* diode behaves more like a variable resistor. Because of the matching circuits for input and output and the bias network, most devices operate in a limited frequency band. Attenuation from 2 dB to 80 dB is achieved.

Step Attenuator. Step attenuators always use a set of fixed attenuators that are switched into a line by different mechanisms. The steps are mostly 0.1 dB, 1 dB, and 10 dB. The 0.1 dB steps generally cover a range of 1.1 dB, the 1 dB steps a

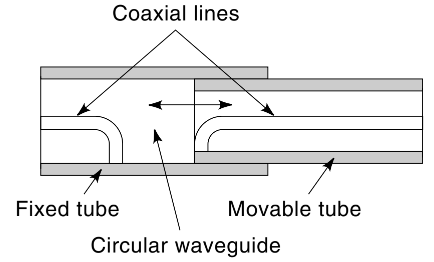

Figure 9. Principle of a piston attenuator.

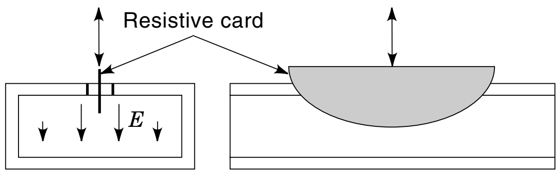

Figure 10. Principle of a waveguide flap attenuator.

range of 11 dB, and the 10 dB steps cover a range up to 110 dB. The step attenuator has excellent repeatability, covers a wide frequency range (e.g., dc to 26.5 GHz), has a good impedance match, and mostly has a flat frequency response of the attenuation value.

In the turret-type coaxial attenuator a set of coaxial fixed attenuators is placed in a cylindrical arrangement. With a rotary motion the different elements (e.g., 0 dB, 10 dB, 20 dB, . . .) are switched between the junctions of the transmission line.

Another type of step attenuator uses a variety of fixed attenuation elements. The different attenuation elements are cascaded by switches or bypassed. The switches may be activated manually or electrically.

Waveguide Attenuator

Waveguide attenuators work mostly in the entire usable waveguide bandwidth, which is not quite half an octave. To attenuate a wave propagated in a waveguide, either the electric or the magnetic field or even both are influenced. As an example, a resistive card inserted into the waveguide parallel to the E-field attenuates it. Another technique uses lossy walls that influence the current in the waveguide wall. Most of these attenuators are not phase-invariant.

Fixed-Value Waveguide Attenuator. The waveguide flap attenuator (Fig. 10) and the side-vane attenuator (Fig. 11) (7) are very popular.

The flap attenuator is based on a resistive card inserted in the center of the waveguide parallel to the E-field. The more the card dives into the waveguide, the more the E-field is weakened, and therefore attenuation increases. A smooth card shape is chosen to minimize the reflection caused by the discontinuity.

The side-vane attenuator (Fig. 11) influences the E-field similarly. The vane is always completely inside the waveguide, but it uses the fact that the E-field varies along the broad side. For the most popular TE_{10} mode, the E-field is zero at the side wall and has its maximum in the center of the waveguide. Therefore the position of the resistive card defines the attenuation value. A smooth shape minimizes the reflection of the discontinuity.

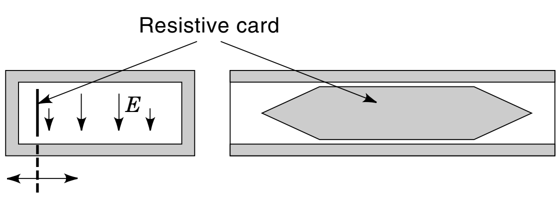

Figure 11. Principle of a side-vane attenuator.

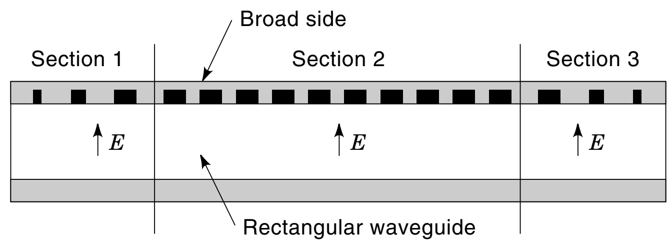

Figure 12. Lossy-wall attenuator.

Several constructions of lossy-wall attenuators exist. One version is shown in Fig. 12 (14).

Section 2 with equally spaced slots filled with a lossy material defines the attenuation. Sections 1 and 3 are configured to minimize the reflection due to the discontinuity in the wall. The lossy-wall attenuator withstands high power because the dissipated heat is transferred to any cooling system.

Variable-Value Waveguide Attenuator

Flap and Side-Vane Attenuator. By adding a mechanism that changes the position of the resistive card, the fixed-value-flap and side-vane attenuator are easily transformed into a variable-value attenuator. It is often used as a settable attenuator.

Rotary-Vane Attenuator. The rotary-vane attenuator was invented in the early 1950s by E. A. N. Whitebread (Elliot H. Brothers, London) and A. E. Bowen (Bell Telephone Laboratories). It was proposed and developed as a precision waveguide attenuator (15–19). The rotary-vane attenuator consists of three sections of waveguide that have a resistive film spanned across the waveguide, as shown in Fig. 13. The middle section has a circular cross section and can be rotated with respect to the two fixed-end sections. Figure 13 illustrates the principle of a rotary-vane attenuator. For clarity, the transitions from a round to a rectangular waveguide at both ends are omitted.

The electric field is perpendicular to all resistive films whenever the films are aligned. In this case no current flows in the resistive film, and therefore no attenuation occurs. If the center part is rotated by an angle θ, the component $E_{\sin\theta}$ in θ produce a current flowing in the resistive film and are absorbed. Thus the resulting attenuation is given by

$$A(\mathrm{dB}) = -40\log(\cos\theta) + A_0 \tag{22}$$

The rotary vane attenuator has the following advantages:

- The attenuation is almost independent of the frequency.
- The phase shift is very small. The phase variations are smaller than 1° up to 40 dB attenuation.
- The input and output VSWRs are very low under all conditions.
- The attenuation is not sensitive to the resistive film as long as its attenuation is high enough.
- The attenuation is not sensitive to temperature changes.

Rotary vane attenuators are commercially available for most of the known waveguide bands. They typically have an accuracy of 2% of the reading in decibels or 0.1 dB, whichever is greater.

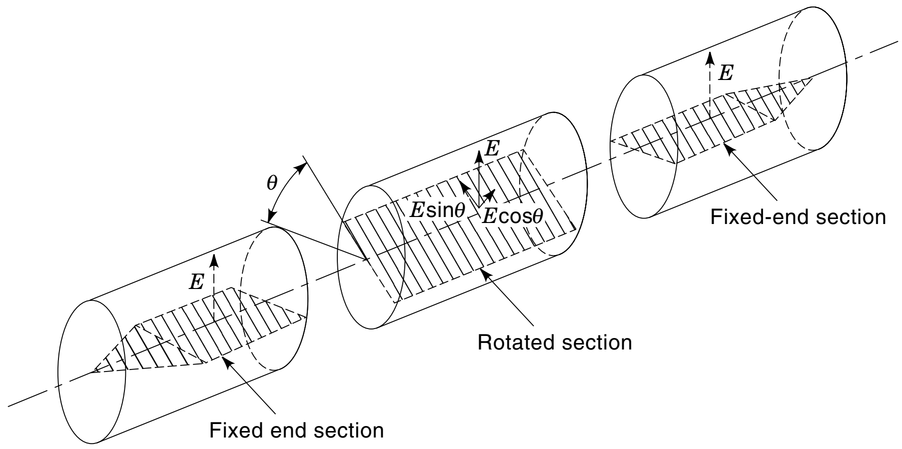

Figure 13. Principle of a rotary-vane attenuator.

Attenuator for Optical Fibers

Attenuators have to be adapted to an optical fiber system. Therefore different attenuators for single-mode or multimode applications are available and mostly operate within one or two wavelength windows. Various attenuation techniques are used to reduce the transmitting light, such as lateral or axial displacement of the fibers or optical prisms, and inserting absorbing filters.

Fixed- or Adjustable-Value Attenuator. A pair of lenses is used in most fiber optical attenuators to collimate the light of the input fiber and to refocus it to the output fiber. Any attenuation mechanism, such as absorbing filters or absorbing glass with variable thickness can be inserted into the optical beam path. Attention has to be given to the attenuation mechanism so that there is very little polarization-dependent loss. Fixed-value attenuators are commercially available for a range of 3 dB to 40 dB with an accuracy of 0.5 dB to 1 dB.

Variable-Value Attenuator. The reflection type variable attenuator often combines a series of 10 dB steps for the high values and a continuous variable attenuation of up to 10 dB or 15 dB. Figure 14 shows the basic configuration of an optical section (20).

A rod lens collimates the light of the fiber into a spatial beam that passes two neutral density filters (ND-filter). The second rod lens focuses the spatial beam into the output fiber. The ND-filter must have high uniformity, little attenuation change with time, and flat spectral transmittance. This is achieved by vacuum-depositing Ni and Cr alloys onto a glass substrate. The ND-filters are the reflecting type. To avoid multiple reflections and to ensure that the light is not reflected into the input lead, the two filters are inclined at a small angle with respect to the optical axis.

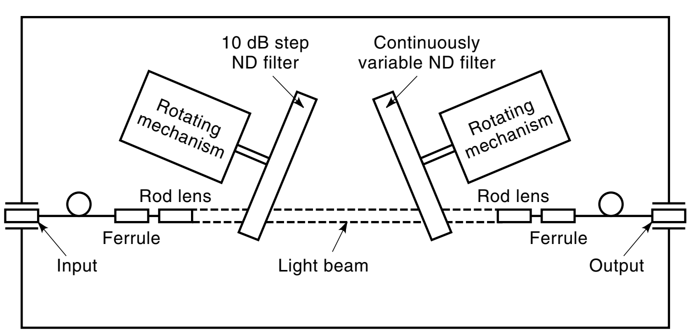

Figure 14. Basic configuration of an optical section.

Commercially available attenuators of this type have an insertion loss of about 3.5 dB, a range of up to 65 dB, and an accuracy of about ±0.5 dB per 10 dB. They are available for wavelengths of 850 nm, 1300 nm, and 1550 nm.

Calculable Attenuation Standards

Many attenuators have been described in the previous sections, but only a few are suitable as attenuation standards. An attenuation standard is a device that can be traced to the SI units by an unbroken chain. The application of the described standards depend on the frequency band and the technique used in the measurement system.

Kelvin–Varley Divider. The Kelvin–Varley divider (KVD) was described for the first time by Varley in 1866 (21). It is a resistive voltage divider and operates from dc up to several hundred kilohertz. Figure 15 is an example of a four-decade Kelvin–Varley divider.

Each decade consists of eleven equal resistors except for the last decade which has only ten. The decades are connected by switches that always span two resistors. The value of the resistors of each following decade is reduced by a factor of 5. The four-decade Kelvin–Varley divider allows varying the output-to-input voltage ratio from zero to one in steps of one part in 10^4. The unloaded KVD has a constant input impedance that is independent of the switch setting whereas the output resistance varies with the setting. The original type of KVD (Fig. 15) requires either very large or very small resistance values because each decade needs five times larger values. Due to stray capacitance, the divider reacts similarly to an RC-filter. For example, a 100 kΩ input impedance limits the 3 dB bandwidth to about 100 kHz. To avoid large resistance values, modified constructions with a resistor shunting the decades have been developed.

Two major errors determine the accuracy: deviations of the resistors from nominal values and the resistances of the switch contacts and leads. The first three or four decades are the most sensitive, and therefore these resistors often are ad-

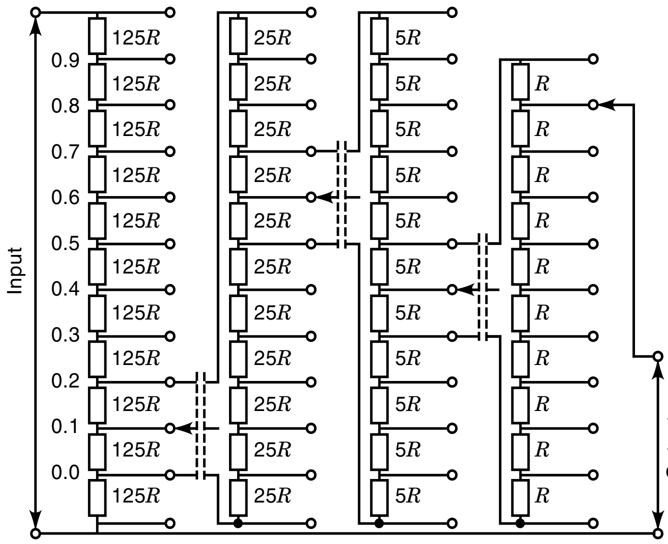

Figure 15. Principle of a four-decade Kelvin–Varley divider.

justable. Several calibration techniques have been developed and are described in the literature (22,23).

Today commercially available Kelvin–Varley dividers have up to seven decades, have an absolute linearity of ±1 part in 10^7, and long term stability of ±1 part in 10^6 per year.

Inductive-Voltage Divider. The inductive-voltage divider (IVD), also called a ratio transformer, is an exceptionally accurate variable attenuation standard. It consists of a number of very accurately tapped autotransformers. The autotransformers are connected together by high quality switches. The IVD operates from 10 Hz to about 100 kHz, and the greatest accuracy is achieved at about 1 kHz. In 1962 Hill and Miller (24) described a multidecade IVD with seven decades and a resolution of 1 part in 10^7. Figure 16 shows the principle of a seven-decade IVD with a setting of 0.4324785. The output-to-input voltage ratio can be set from zero to one.

The tapped autotransformers are constructed by winding exactly equal lengths of copper wire on a high permeability toroidal core. A superalloy having an extremely high permeability (>100,000) and low hysteresis loss is preferred as a core material. For an exact division of the tapped autotransformer, it is not necessary to have a 100% coupling between the ten inductors (4). But the 10 self-inductances and the 45 mutual inductances have to be exactly equal.

The following error sources limit the accuracy of IVDs:

- inequality in the series resistances and the leakage inductances of the sections in each autotransformer
- inhomogenities in the magnetic cores
- distributed admittances between the windings
- internal loading caused by the later stages
- impedances of the connecting leads and switch contacts
- variations in the input voltage, frequency, and ambient temperature

With careful design the mentioned errors can be minimized. Recently, programmable binary IVDs with 30 bits, a resolution of 1 part in 10^9, and a linearity of 0.1 ppm have been developed (25).

IVDs with eight decades and an accuracy of four parts in 10^8 are commercially available.

Intermediate-Frequency Piston Attenuator. The IF piston attenuator is based on the same principle as the attenuator previously described for RF, but it is designed to operate at a specific, fixed frequency, mostly 30 MHz or 60 MHz. As Eq. 21 shows, attenuation depends on the cutoff wavelength λ_c, the free-space wavelength λ, and the displacement of the two coils. The waveguide dimensions, which can be determined, define the cutoff wavelength, and the displacement can be measured very precisely. Therefore the IF piston attenuator is used as a calculable standard. Figure 17 shows a simplified diagram of an IF piston attenuator.

The standard IF piston attenuator consists of a high-precision circular cylinder that has excellent conductivity, a fixed coil, and a movable coil mounted on a piston. The piston attenuator operates in the H_{11} (TE_{11}) mode that has the lowest attenuation. A well-designed metal strip filter in front of the

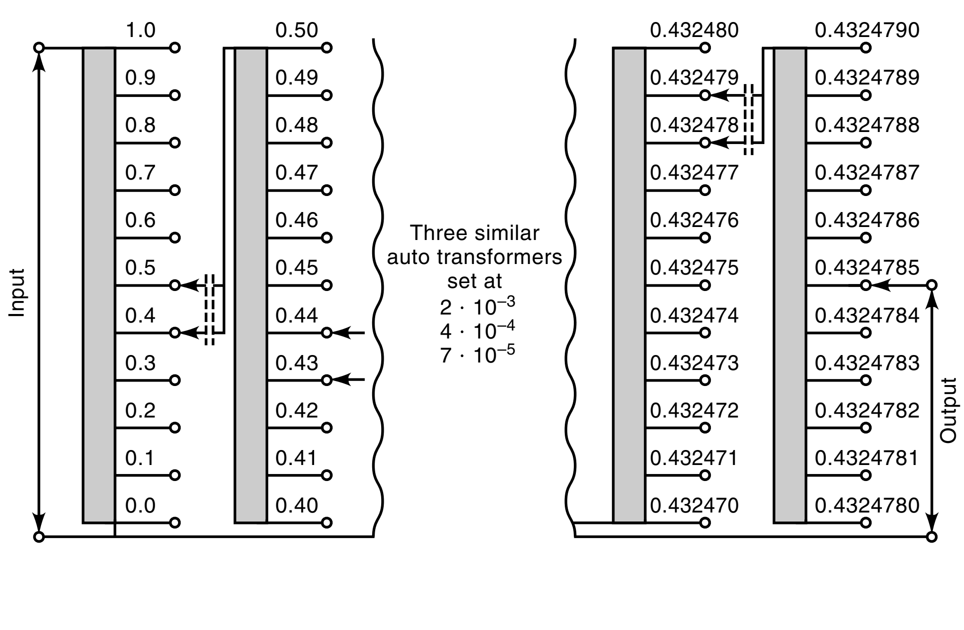

Figure 16. Principle of a seven-decade IVD.

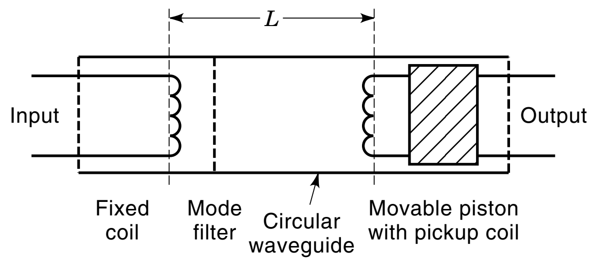

Figure 17. Simplified IF piston attenuator.

fixed coil attenuates the higher modes. To allow smooth movement and to avoid any scratches, the plunger carrying the moving coil is insulated. Equation 23 expresses the attenuation per unit length more precisely:

$$A = \frac{s_{11}}{r}\sqrt{1 - \left(\frac{\lambda_c}{\lambda}\right)^2 \cdot \epsilon - \frac{\delta}{r}} \tag{23}$$

in nepers per unit length, where $\lambda_c = 2\pi r/s_{11}$, λ_c is the cutoff wavelength, λ is the free-space wavelength, s_{11} the first zero of the Bessel function $J_1 = 1.8411838$, r the radius of the cylinder, and δ is the skin depth.

Highly accurate standard attenuators use a laser interferometer to accurately determine the displacement of the coil. Yell (26,27) and Bayer (28) developed extremely accurate IF piston attenuators with a dynamic range of 120 dB, a resolution of 0.0001 dB, and an accuracy of 0.0002 dB/10 dB over the linear range of 90 dB.

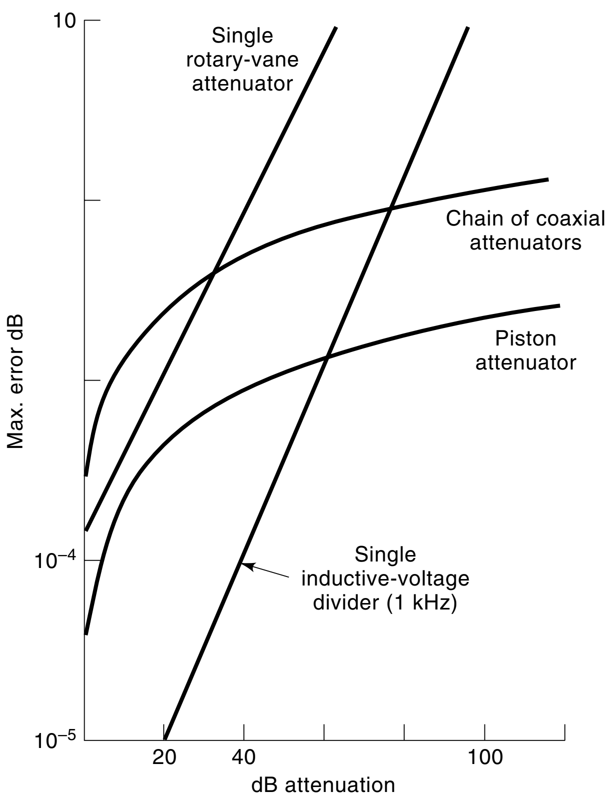

Figure 18. Comparison of attenuation standards.

Rotary-Vane Attenuator. The principle of the rotary-vane attenuator is described in the section Variable Waveguide Attenuator. Because the attenuation is given by the equation

$$A(\mathrm{dB}) = -40\log(\cos\theta) + A_0 \tag{24}$$

where A_0 is the insertion loss at a setting of $\theta = 0$, the device can be used as a calculable primary standard.

The rotating angle θ of the center vane has to be determined very precisely, especially for higher attenuation values. As an example, a rotational angle accuracy of $\pm 0.001°$ results in an attenuation accuracy of ± 0.01 dB at a setting of 60 dB. Especially precise optical readouts have been developed by national standards laboratories (29–31) to allow an angular resolution of $\pm 0.001°$. Following are the main error sources for precision rotary-vane attenuators:

misalignment of the end vanes
insufficient attenuation of the central vane
incorrect readout of the rotational angle
eccentricity of the rotor
leakage of the rotating joints
internal reflections at the ends of the three vanes

Careful design of the attenuator results in an accuracy of ± 0.0015 dB up to 16 dB at 10 GHz.

Comparison of Attenuation Standards. The attenuation standards mentioned previously are used in various precision measurement systems, such as RF-, IF- or LF-substitution. The standards have very different accuracy depending on the attenuation setting. Figure 18 shows a comparison of different precision attenuation standards used in national metrology laboratories (32).

Optical Attenuation Standards. Imamura (33) shows one solution of a calculable optical attenuation standard that is used to calibrate precision attenuators. The key element is a rotating disk with a well-defined opening. The device operates as an optical chopping system (Fig. 19).

As long as the response of the detector is slow compared to the rotational speed ω, the ratio P_1 to P_0 defines the attenuation. In this case the attenuation depends only on the opening angle θ (in radians) and is given by the following equation:

$$A = -10 \cdot \log\frac{P_1}{P_0} = -10 \cdot \log\frac{\theta}{2\pi} \tag{25}$$

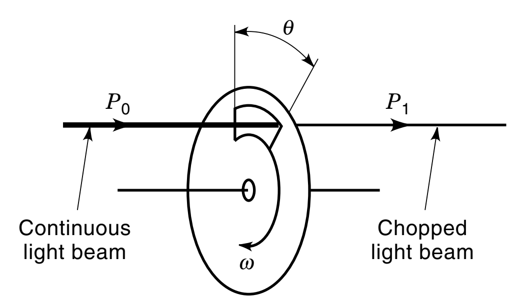

Figure 19. Principle of an optical chopping system.

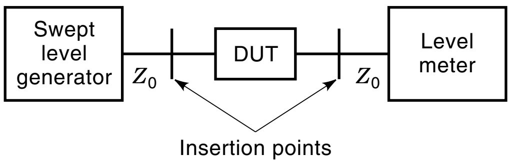

Figure 20. Principle of a direct measurement system.

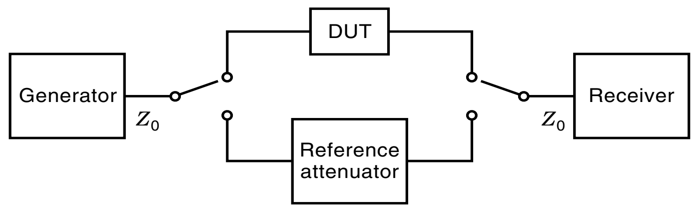

Figure 21. Principle of a LF-substitution method.

An opening angle of 36° defines an attenuation of 10 dB. Special care has to be paid to the diffraction of light at the edges of the disk openings and the stability of the light source and the sensor. The overall accuracy is estimated to be ±0.008 dB for 10 dB attenuation.

MEASUREMENT OF ATTENUATION

Various kinds of measurement systems are used depending on the frequency range, the type of attenuator, the required accuracy and the available standards. Most of the modern attenuation measurement systems are computer- or microprocessor-controlled. They use the same principle as the manual systems but operate much faster. If maximum accuracy is required, manually controlled measurement systems are often preferred.

Low-Frequency Measurement Systems

Low frequency attenuation measurements are used mainly in communication systems where voice, video and data have to be transmitted with as little distortion as possible. Dedicated test systems have been developed for testing and adjusting the communication systems working either with coaxial lines (50 Ω or 75 Ω) or balanced lines (124 Ω, 150 Ω, or 600 Ω).

Direct Measurement. Operation of communication systems requires a great number of test systems for which low-cost test systems that are easily handled were developed. The systems are based on current, voltage, or power measurement and operate in a frequency band from 200 Hz up to 30 MHz. The test system (Fig. 20) consists of a tuneable generator with a known constant output level and a wideband voltmeter or a high-sensitivity, selective superheterodyne receiver.

Many test systems can be switched to operate in either coaxial-line (50 Ω or 75 Ω) or balanced line (124 Ω, 150 Ω, or 600 Ω) configuration. In the balanced-line mode the test systems have a limited frequency range of 200 Hz to several MHz depending on the impedance selected. In the selective-level meter mode, bandwidths of 25 Hz to 3.1 kHz are used, and the dynamic range achieved is on the order of 80 dB. The attenuation measurement accuracy in the frequency range indicated is about 1 dB.

Low-Frequency Substitution Method. The LF-substitution method is based on a precisely calibrated low-frequency reference attenuator used in a parallel or a serial configuration (Fig. 21).

Because the attenuation of the device under test (DUT) is compared with that of the reference attenuator, neither the output level of the generator nor the absolute level indication of the receiver have to be known. The only requirements are that generator and receiver remain stable during measurements. The accuracy is determined mainly by the calibration of the reference attenuator.

Radio Frequency and Microwave

In radio frequency and microwave many different measurement principles are known. They all have their own characteristics: one is meant to measure low values of attenuation, another to measure high values, a third to achieve highest accuracy. The most popular measurement principles are discussed in the following sections.

Power Ratio Method. The power ratio method (4,40) (Fig. 22) is very simple for measuring attenuation. It is commonly used as long as maximum accuracy is not required.

The method is based on the linearity of the power meter or the receiver used. First the power P_1 of the generator is measured without the device under test (DUT) and then P_2 is measured with the DUT inserted. The attenuation of the DUT is calculated by the ratio of P_2 to P_1:

$$A(\mathrm{dB}) = 10 \log \frac{P_2}{P_1} \tag{26}$$

To measure attenuation, the insertion points have to be matched either by tuners or matching pads. The square law characteristic of the power sensors and the noise limit the dynamic range to about 40 dB. If a tuned receiver is used instead of a power meter, the measurement range is extended to about 100 dB.

Several error sources influence the accuracy:

- the stability of the generator and the detector system
- the frequency stability of the generator
- the matching at the insertion points

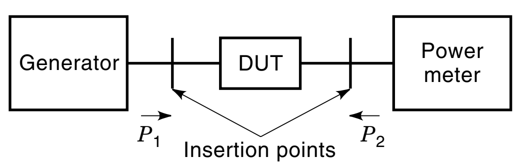

Figure 22. Principle of the power ratio method.

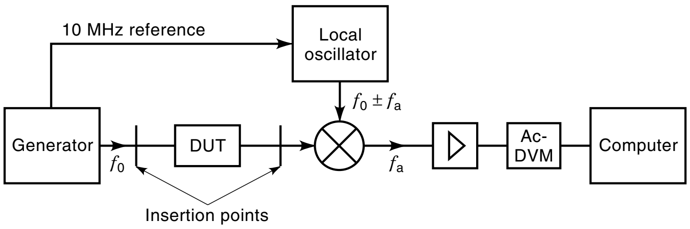

Figure 23. Principle of the voltage ratio method.

- the square law region of the detector system
- the crosstalk for high attenuation measurement

Commercially available systems using a tuned receiver achieve a measurement uncertainty of 0.1 dB at 50 dB attenuation. These systems are easily automated by controlling the instruments with a computer.

In national standards laboratories very sophisticated systems have been developed resulting in an accuracy of 0.06 dB at 50 dB attenuation (34,35).

Voltage Ratio Method. The voltage ratio method makes use of high resolution ac-digital voltmeters (ac-DVM) available now. Because the ac-DVMs work only up to several MHz, the RF signals have to be down-converted to low frequency. Figure 23 shows the principle of a voltage ratio system working at an audio frequency of 50 kHz.

If a synthesizer locked to the same reference frequency is used as a signal generator and local oscillator, a very stable audio frequency f_a (e.g., 50 kHz) is generated. The audio frequency signal is amplified and measured with an ac-DVM. If U_1 is the voltage measured with the two insertion points clamped together and U_2 is the voltage with the DUT inserted, the attenuation is given by

$$A(\mathrm{dB}) = 20\log\left(\frac{U_2}{U_1}\right) + C \qquad (27)$$

where C is the correction factor in decibels for the nonlinearity of the amplifier and the DVM.

The dynamic range of the direct system is about 20 to 30 dB. More sophisticated systems achieve an uncertainty less than 0.001 dB for 20 dB attenuation. By adding a gauge block technique, for example, a calibrated step attenuator (10, 20, 30, 40, 50, 60, 70 dB) in series with the DUT in the RF path, the range is extended to 90 dB with excellent accuracy of 0.001 dB (32).

The error sources which limit the measurement uncertainty are

- the matching of the insertion points
- the generator output level stability
- the AF-amplifier stability
- the AF-amplifier and ac-DVM linearity
- the mixer linearity
- the gauge-block attenuator stability and reproduceability
- the crosstalk for high attenuation measurement

IF-Substitution Method. The IF-substitution method (4,40) (Fig. 24) gives good accuracy, operates over a large dynamic range, and is used up to very high frequencies. Most systems operate in a parallel substitution mode.

The signal passing through the DUT is mixed to an IF of 30 or 60 MHz. This signal is compared with the signal of the 30 MHz reference oscillator and the standard attenuator by a narrowband 30 MHz receiver (mostly with synchronous detection). In a first phase the insertion points are clamped together, and the standard attenuator is adjusted until there is no switching signal (i.e., 1 kHz) detectable any longer. The reading A_1 of the standard attenuator is taken. In a second phase the DUT is inserted, the standard attenuator is adjusted so that the signal of the standard attenuator equals the signal of the mixer, and the reading A_2 is taken. The attenuation of the DUT is given by the difference A_2 minus A_1 between readings.

A piston attenuator, an inductive-voltage divider, or a high-precision resistive attenuator can be used as a standard attenuator.

In national standards laboratories very high-precision piston attenuators with a resolution of 0.0001 dB over a 100 dB range have been used in a parallel substitution system. The accuracy achieved is better than 0.001 dB per 10 dB step (27,32,36).

Accuracy of about 0.002 dB and a dynamic range of 100 dB have been achieved by using a seven-decade 50 kHz inductive voltage divider in a parallel substitution system (37).

Weinert (38) proposed a parallel IF complex vector substitution system using a high precision IF attenuator. The system has a single-step dynamic range of 140 dB and a display resolution of 0.001 dB.

The following error sources limit the accuracy and the dynamic range:

- the matching at the insertion points
- the level stability of the signal source
- the mixer linearity
- the noise balance
- the level stability of the IF reference oscillator
- the standard attenuator resolution and stability
- the crosstalk for high attenuation measurement

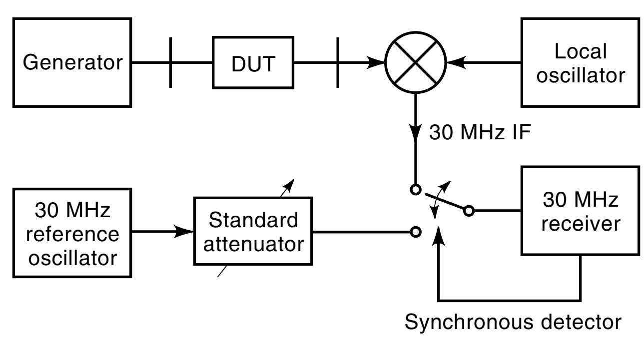

Figure 24. Principle of the IF-substitution method.

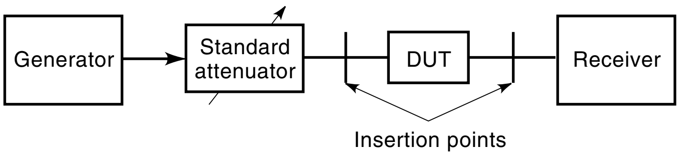

Figure 25. Principle of the series RF-substitution method.

RF-Substitution Method. In the RF-substitution method (4,40) (Fig. 25), the reference standard attenuator and the DUT operate at the same frequency. Because the attenuation of the reference standard is compared either in a series or in a parallel substitution system with the DUT, the results are independent of the receiver characteristics. A rotary-vane attenuator, a piston attenuator, or a chain of well-matched and precisely calibrated attenuators (e.g., step attenuator) is used as a reference standard.

In the first step the insertion points are clamped together, and the reference standard is adjusted to a value A_1 according to the estimated attenuation of the DUT. The receiver shows the reading U_1. In the second step the DUT is inserted, and the reference standard is adjusted to get the same reading U_1 at the receiver A_2. The attenuation of the DUT is calculated as the difference beween the two decibel readings of the reference attenuator, A_1 minus A_2.

Scalar Measurement. All of the attenuation measurement systems described in the previous sections provide scalar measurements. There are many commercial scalar network analyzers available (Fig. 26) (8,39). These analyzers measure the input reflection and the attenuation of the device under test. Because mostly wideband detectors are used, only the magnitude of two quantities can be determined.

The signal of the sweep generator is divided by a power splitter or a directional coupler into reference and measurement paths. The directional bridge or coupler measures the reflected wave of the DUT. The analyzer forms the ratio A/R which is proportional to the input reflection coefficient of the DUT. Using a third detector, the attenuation is measured by calculating the ratio B/R. Most scalar network analyzers are microprocessor- or computer-controlled and offer simple correction methods. The calibration for reflection measurements is frequently done by using open and short circuits, and a connect through normalization is used for the transmission path. Because these analyzers are broadband systems, they operate very fast and are easily expandable to highest frequencies. Commonly used scalar network analyzers operate from 10 MHz to 18 GHz or 26 GHz, and often their frequency range can be extended to 50 GHz in coaxial lines and to 110 GHz in wave guides. The dynamic range is limited to about 75 dB by the square law characteristic of the detectors and noise. The measurement accuracy achieved is quite reasonable for example, 0.6 dB measuring a 30 dB attenuator. The insertion points have to be well matched.

The following errors influence the measurement uncertainty:

the harmonics of the sweep generator;
the matching of the insertion points;
the square law characteristic of the detectors; and
the sweep generator level stability.

Vector Measurement. Vector measurements enable characterising a two-port circuit completely. In addition to the magnitude, the phase of the scattering parameters is also determined. There are two major concepts for measuring the complex parameters of a two port device: the vector network analyzer and the six-port technique.

Modern vector network analyzers (8,39,40) measure all four scattering parameters: s_{11}, s_{21}, s_{12}, and s_{22} without the necessity of turning the DUT around. Therefore they are symmetrical (Fig. 27) and measure in both directions.

The basic concept looks similar to that of the scalar network analyzer. The signal of the generator is divided into reference and measurement paths. In forward measurements, the directional bridge A determines the reflected signal, bridge B determines the transmitted signal, and vice versa for the reverse case. Instead of using diode detectors, the signals are down-converted to an intermediate frequency and analyzed in magnitude and phase. Synthesized sweep generators and synchronous detection are being used to obtain high accuracy for magnitude and phase measurements. Because the complex signals are measured, the main errors due to component imperfections may be corrected. Frequently a 12-term error model is applied to correct the source and load match, the bridge characteristics, the transmission leakage cross talk and down-converter characteristics. In the first phase well-known standards (e.g., open, short, line) are measured, and the 12 error parameters are determined. In the second phase the DUT is measured and the data corrected according to the calculated error terms. Several different

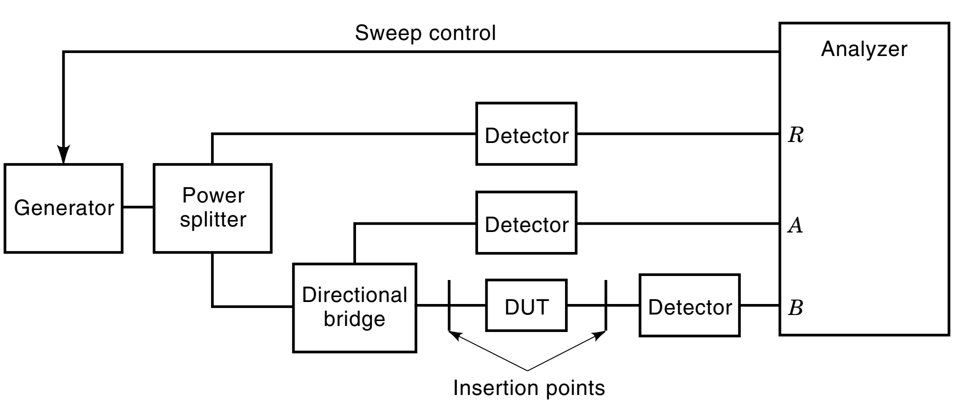

Figure 26. Principle of a scalar network analyzer.

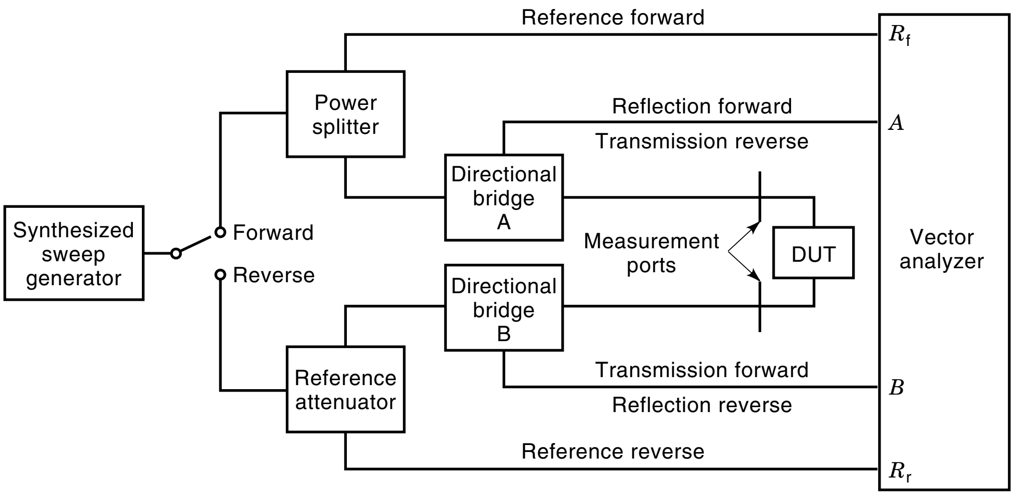

Figure 27. Principle of a vector network analyzer.

techniques for measuring the error parameters are used, such as open-short-load, transmission-reflect-line, line-reflect-line, etc. Each technique uses different kinds of reference standards, such as short and open circuits, well defined lines, known loads.

Excellent performance is achieved by using the 12-term error correction technique. For example, at 20 GHz, load and source match better than −38 dB return loss, transmission tracking is better than 0.06 dB and cross talk is less than −104 dB. As a result a 30 dB attenuator can be measured at 20 GHz with an uncertainty of 0.07 dB.

Vector network analyzers are commercially available in coaxial configurations in frequency bands from about 100 kHz to 50 GHz and in waveguides up to 110 GHz. Some specially dedicated systems operate in waveguides up to 1000 GHz.

The measuring uncertainty is defined mainly by the following parameters:

- accuracy of the reference standards
- stability of the generator and of the detection system
- stability of the connection cables
- repeatability of the connectors
- accuracy of the built-in software to calculate the error parameters and DUT scattering parameters

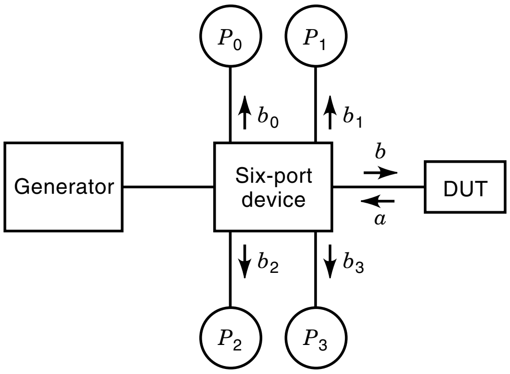

Figure 28. Principle of six-port technique for reflection measurement.

The six-port technique is another method for measuring the complex scattering parameters of a device. The magnitude and the phase of the signal are calculated from four scalar power measurements made with detectors arranged as shown in Fig. 28 (8,40).

The four power sensors gather enough information to calculate the magnitude and phase of the reflection of the DUT and the power launched into it. The calibration of the six-port device is rather complicated because a set of quadratic equations has to be solved. The quadratic equations can be linearized and solved for both calibration and measurement (8,40).

The simplicity of the detection system is an advantage of the six-port device especially for wideband applications and very high operating frequencies. Compared to the vector network analyzer, the six-port device requires more calibration and more complicated mathematics.

Two six-port devices connected in the configuration shown in Fig. 29 are required to provide attenuation measurements.

The dividing circuit includes phase adjustments to obtain different ratios b_1/b_2 at the terminals of the DUT. Using state-of-the-art power sensors the dynamic range of a dual six-port device is as large as 60 dB.

To achieve maximum accuracy, through connection, reflection line TRL-calibration is frequently used. Because the six-port device determines the complex parameters during the calibration process, the test ports appear well matched. The measurement uncertainties are primarily limited by the calibration standards, mainly the reflection standard (short or

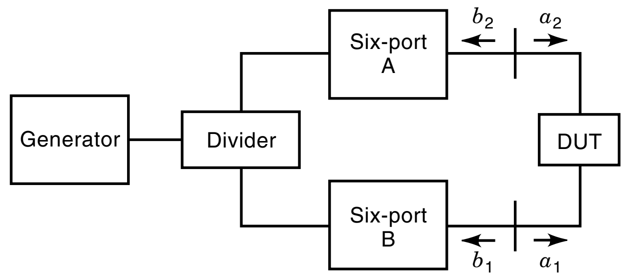

Figure 29. Principle of a dual six-port for s-parameter measurement.

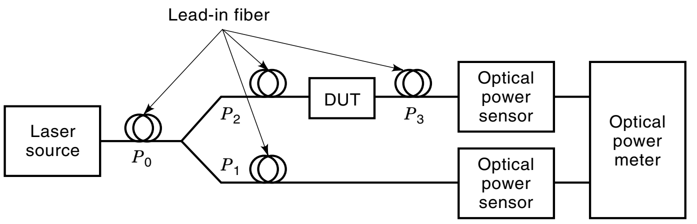

Figure 30. Principle of the insertion-loss method.

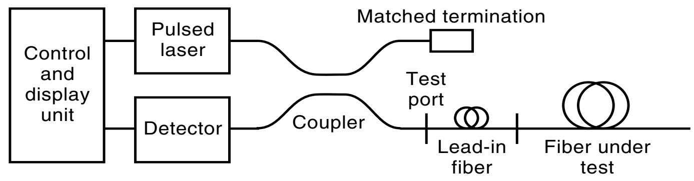

Figure 32. Principle of an optical time-domain reflectometer.

open). Real-time operation is limited by the computing time and the response time of the power sensors.

Fiber Optics

Three main methods (41,42) are used for attenuation measurements: the insertion loss technique, the cut-back technique, and the backscattering method. The first two methods perform two-point (end to end) measurements and the last performs a one-ended characterization. Some of the methods are standardized (43,44).

Insertion Loss Method. The insertion loss technique consists of a stable laser source and a stable, accurate, optical power meter. The power P_2 of the laser source is sent into the DUT (e.g., an optical fiber), and the power P_3 is measured at the far end. The attenuation is given by the ratio of the two power levels as

$$A(\mathrm{dB}) = 10\log\left(\frac{P_3}{P_2}\right) \tag{28}$$

To achieve more accurate measurements in the first phase, the power of the source is directly measured and is remeasured in the second phase with the DUT inserted. More sophisticated measuring systems use a configuration shown in Fig. 30.

A second power sensor measures the power level of the source instantaneously by a power divider. In this configuration the power stability of the source is less important because P_1 is always used as a reference. By using cooled detectors, a dynamic range up to 90 dB is achieved.

The accuracy of the measurements are determined by the following factors:

- the power level and wavelength stability of the source
- the calibration and stability of the power sensors
- the reproduceability of the connectors
- the linearity of the detectors

The measurement uncertainties for the insertion-loss technique are on the order of 0.9 dB including the connector reproduceability. Sophisticated systems reach over a limited dynamic range of 50 dB and uncertainty of 0.2 dB.

Cut-Back Method. The cut-back method (41,45) (Fig. 31) is the most accurate technique, but it is destructive. This method was developed to measure the attenuation of fibers as a function of the wavelength. Using a light source combined with a monochromator, a fiber can be tested at any wavelength from 800 nm to 1600 nm with a spectral width of 3 nm. The light from the source is projected into the fiber by a lens.

The power $P_2(\lambda)$ is measured at the far end of the fiber (test length l_t) by using a cooled detector. Then the fiber is cut back to a short length of 2 m to 3 m without changing the projecting conditions, and the power $P_1(\lambda)$ is recorded. If the power loss in the short length of fiber is assumed to be negligible, the attenuation is given by the following equation:

$$A(\lambda) = 10\log[P_2(\lambda)/P_1(\lambda)] \tag{29}$$

Assuming a uniform fiber, the attenuation coefficient per unit length of the fiber is given by

$$\alpha(\lambda) = \frac{A(\lambda)}{(l_t - l_r)} \tag{30}$$

where l_t and l_r are given in kilometers. The achieved uncertainty for cable length of several kilometers is about 0.02 dB/km for multimode fibers and 0.004 dB/km for single mode.

Backscattering Method. The backscattering method is a one-ended measurement based on Rayleigh scattering in an optical fiber (41,46). Figure 32 shows the principle of an optical time-domain reflectometer (OTDR).

A laser pulse is projected into the fiber by a coupler, and the backscattered power is measured. The backscattered power is related to the attenuation loss of the fiber and the measured time delay is related to the distance in the fiber. The attenuation is calculated by using two values of the backscattered power at different time delays (different locations along the fiber). The OTDR has the advantage of providing attenuation and reflection information along the fiber. A typical recording is shown in Fig. 33.

The length of the pulse is responsible for the dead zone where no measurement is possible. A lead-in fiber allows masking the dead zone. From the measured data details in the fiber path, such as connector loss or splice loss, irregularities of attenuation and defects are be analyzed.

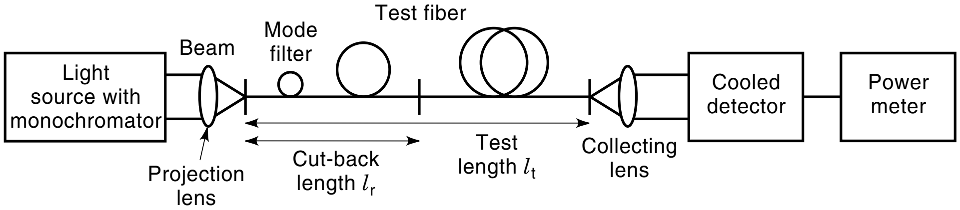

Figure 31. Principle of the cut-back method.

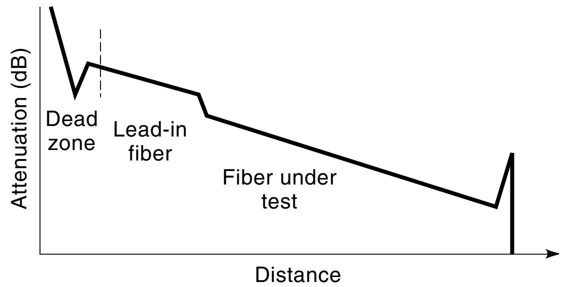

Figure 33. Typical backscattering signature of a fiber.

Commercially available OTDRs have a dynamic range of about 35 dB and cover distances up to 65 km depending on the fiber loss. A well-calibrated OTDR can produce a measurement uncertainty of about 0.02 dB/km.

ERRORS AND UNCERTAINTIES IN ATTENUATION MEASUREMENTS

Whenever measurements are made, the results differ from the true or theoretically correct values. The differences are the result of errors in the measurement system, and it should be the aim to minimize these errors. In practice there are limits because no measurement instruments operate perfectly. A statement of measurement uncertainty reflects the quality of the measured results, and it has to be accompanied by a statement of confidence.

The International Committee for Weights and Measures (CIPM) (47) has published a guide for expressing uncertainty in measurements which has been adopted by the European Cooperation for Accreditation of Laboratories (EA) (48). According to the guide, uncertainty is grouped in two categories: Type A and Type B.

Type A evaluation is the result of statistical analysis of a series of repeated observations and therefore includes random effects.

Type B evaluation is by definition other than Type A, for example, judgment based on data of calibration certificates, experiences with instruments, and manufacturers' specifications.

Type A Evaluation of Uncertainty Components

Random effects result in errors that vary unpredictably. For an estimate of the standard deviation $s(q_k)$ of a series of n readings, q_k is obtained from

$$s(q_k) = \sqrt{\frac{1}{(n-1)} \sum_{k=1}^{n} (q_k - \overline{q})^2} \tag{31}$$

where $\overline{q}$ is the mean of n measurements.

The random component of uncertainty is reduced by repeating the measurements. This yields the standard deviation of the mean $s(\overline{q})$

$$s(\overline{q}) = \frac{s(q_k)}{\sqrt{n}} \tag{32}$$

The standard uncertainty of the input estimate $\overline{q}$ is the experimental standard deviation of the mean (for $n \geqslant 10$)

$$u(\overline{q}) = s(\overline{q}) \tag{33}$$

Type B Evaluation of Uncertainty Components

Systematic effects that remain constant during measurements but change if the measurement conditions are altered cannot be corrected and therefore contribute to uncertainty. Other contributions arise from errors that are not possible or impractical to correct for, such as from calibration certificates or manufacturers' specifications. Most of these contributions are adequately represented by a symmetrical distribution. In RF metrology three main distributions are of interest: normal, rectangular, and U-shaped.

Normal Distribution. Uncertainties derived from multiple contributions are assumed to be normally distributed. Accredited calibration laboratories issue calibration certificates calculated for a normal distribution and a minimum level of confidence of 95% (approximate coverage factor $k = 2$). The standard uncertainty associated with the estimate x_i is given by

$$u(x_i) = \frac{\text{uncertainty}}{k} \tag{34}$$

Rectangular Distribution. This means that there is equal probability that the true value lies between limits. This is the case for most manufacturers' specifications that give a semirange limit a_i:

$$u(x_i) = \frac{a_i}{\sqrt{3}} \tag{35}$$

U-Shaped Distribution. This distribution is applicable to mismatch uncertainty (49). Because the phases of the reflection coefficients (of source, DUT, load) in scalar measurement are not known, the mismatch loss has to be taken into account as an uncertainty. The mismatch uncertainty is asymmetrical to the measured result, and normally the larger of the two limits $M = 20 \log(1 - |\Gamma_G|\,|\Gamma_L|)$ is used. The standard uncertainty is calculated as

$$u(x_i) = \frac{M}{\sqrt{2}} \tag{36}$$

Combined Standard Uncertainty

The combined standard uncertainty for uncorrelated input quantities is calculated as the square root of the sum of the squares of the individual standard uncertainties:

$$u_c(y) = \sqrt{\sum_{i=1}^{m} u_i^2(y)} \tag{37}$$

Expanded Uncertainty

The expanded uncertainty U defines an interval in which there is the true value with a specified confidence level. Normally accredited calibration laboratories are asked to use the

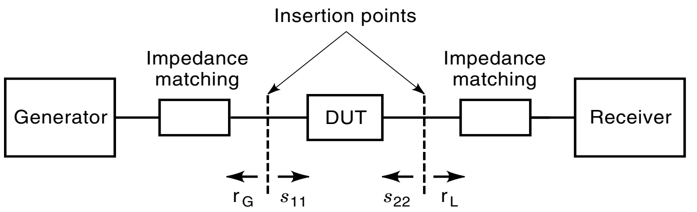

Figure 34. Example of an attenuation measurement system.

coverage factor $k = 2$ (approximately 95% confidence level) giving:

$$U = k \cdot u_c(y)$$

Uncertainty in Attenuation Measurement

Let us assume a simple attenuation measuring setup, shown in Fig. 34, consisting of a generator, two matching circuits and a receiver. In the first phase when the two insertion points are clamped together, the receiver measures $P_1(f)$ (often called a normalization). In the second phase the DUT is inserted, and the receiver reads the values $P_2(f)$.

Attenuation as a function of the frequency is calculated from the ratio of the two sets of readings:

$$A(f) = 10 \log \left[\frac{P_2(f)}{P_1(f)} \right] \tag{38}$$

The following errors contribute to the uncertainty of the measurement:

The statistical errors of n repeated measurements (Type A) are given by the arithmetic experimental standard deviation:

$$s(A) = \sqrt{\frac{1}{(n-1)} \sum_{k=1}^{n} (A_k - \overline{A})^2} \tag{39}$$

($\overline{A}$ is the arithmetic mean of the measurements)

The standard uncertainty is calculated from

$$u_s(A) = s(\overline{A}) = \frac{s(A)}{\sqrt{n}} \tag{40}$$

The generator level stability a_G is taken from the manufacturer's specification and is assumed to be rectangularly distributed. The uncertainty is calculated as follows:

$$u_G = \frac{a_G}{\sqrt{3}} \tag{41}$$

The receiver level linearity and stability a_R is taken from the manufacturer's specification. The uncertainty is calculated as

$$u_R = \frac{a_R}{\sqrt{3}} \tag{42}$$

The noise level of the receiver influences the measurement of high attenuation values. It is given in the manufacturer's specification and contributes to the uncertainty as

$$u_N = \frac{a_N}{\sqrt{3}} \tag{43}$$

The cross talk of the measurement system a_I is determined by measurements and regarded as limits, and therefore contributes to the uncertainty as

$$u_I = \frac{a_I}{\sqrt{3}} \tag{44}$$

Two mismatch losses have to be taken into account, one during the normalization (often also called calibration) phase and the second while measuring the DUT.

Normalization Phase. The maximum mismatch loss (49) is calculated from the reflection coefficients of the source and the receiver as

$$M_C = 20 \log(1 - |r_G||r_L|) \tag{45}$$

As in scalar measurements, the phases of the reflection coefficients are unknown. The mismatch loss contributes to the measurement uncertainty and is normally assumed to be U-shaped distributed:

$$u_C = \frac{M_C}{\sqrt{2}} \tag{46}$$

Measurement Phase. There are two mismatch losses (49) that have to be considered: one between the generator and the input of the DUT and the other between the output of the DUT and the receiver. In addition, for small attenuation values the interaction between the input and the output connection has to be considered. The maximum limits of the mismatch loss which have to be used for the uncertainty are given by

$$M_m = 20 \log \frac{|1 - |r_G s_{11}| - |r_L s_{22}| - |r_G r_L s_{11} s_{22}| - |r_G r_L s_{21} s_{12}||}{1 - |r_G r_L|} \tag{47}$$

The uncertainty is given by

$$u_m = \frac{M_m}{\sqrt{2}} \tag{48}$$

The total uncertainty is calculated either from linear values or from decibel values as long as they are small:

$$u_c(A) = \sqrt{u_s^2 + u_G^2 + u_R^2 + u_N^2 + u_I^2 + u_C^2 + u_m^2} \tag{49}$$

The expanded uncertainty is calculated using a coverage factor $k = 2$ (approximately 95% confidence level) as

$$U(A) = k \cdot u_c(A) = 2 \cdot u_c(A) \tag{50}$$

The uncertainty has to be calculated for all of the measurement frequencies to find the maximum value of the uncertainty.

BIBLIOGRAPHY

1. D. M. Kerns and R. W. Beatty, *Basic Theory of Waveguide Junctions and Introductory Microwave Network Analysis,* New York: Pergamon, 1967.
2. R. W. Beatty, *Applications of Waveguide and Circuit Theory to the Development of Accurate Microwave Measurement Methods,* NBS Monograph 137, Washington, DC: US Government Printing Office, 1973.
3. R. W. Beatty, Insertion loss concepts, *Proc. IEEE,* **52**: 663, 1964.
4. F. L. Warner, *Microwave Attenuation Measurement,* IEE Monograph Series 19, London: Peregrinus, 1977.
5. S. J. Mason, Feedback theory-some properties of signal flow graphs, *Proc. IRE,* **41**: 1144–1156, 1953.
6. N. Kuhn, Simplified signal flow graph analysis, *Microw. J.,* (11): 59–66, 1963.
7. S. F. Adam, *Microwave Theory and Applications,* Englewood Cliffs, NJ: Prentice-Hall, 1969.
8. G. H. Bryant, *Principles of Microwave Measurements,* IEE Electrical Measurement Series 5, London: Peregrinus, 1993.
9. T. S. Laverghetta, *Modern Microwave Measurements and Techniques,* Norwood, MA: Artech House, 1998.
10. *Reference Data for Engineers,* 7th ed., Indianapolis, IN: H. W. Sams, 1985.
11. E. Weber, Precision Metalized Glass Attenuators, *Technique of Microwave Measurements,* MIT Radiation Lab Series, vol. 11, New York: McGraw-Hill, pp. 751–774.
12. S. F. Adam, Precision thin-film coaxial attenuators, *Hewlett-Packard J.,* 12–19, June 1967.
13. C. G. Montgommery, *Technique of Microwave Measurements,* MIT Radiation Lab Series Vol. 11, New York: McGraw-Hill.
14. W. Bolinger, private communication.
15. H. L. Kundsen, Champs dans un guide rectangulaire à membrane conductrice, *L'Onde Electrique,* April 1953.
16. B. P. Hand, A precision waveguide attenuator which obeys a mathematical law, *Hewlett Packard J.,* **6** (5): 1955.
17. G. C. Southworth, *Principles and Applications of Waveguide Transmission,* Van Nostrand: Princeton, NJ: 1950, pp. 374–376.
18. B. P. Hand, Broadband rotary vane attenuator, *Electronics,* **27**: 184–185, 1954.
19. P. F. Mariner, An absolute microwave attenuator, *Proc. IEE,* **109B**: 415–419, 1962.
20. T. Imanura, MN 9002A Standard optical attenuator, *Anritsu Techn. Rev.,* **14**: 32–41, 1991.
21. C. F. Varley, On a new method of testing electronic resistance, *Math. Phys. Sect. Br. Assoc. Adr. Sci.,* 14–15, 1866.
22. M. L. Morgan and J. C. Riley, Calibration of a Kelvin–Varley standard divider, *IRE Trans.,* **I-9** (1): 273–243, 1960.
23. A. F. Dunn, Calibration of a Kelvin–Varley voltage divider, *IEEE Trans. Instrum. Meas.,* **IM-3**: 129–139, 1964.
24. J. J. Hill and A. P. Miller, A seven-decade adjustable-ratio-inductively-coupled voltage divider with 0.1 part per million accuracy, *Proc. IEE,* **109**: 157–162, 1962.
25. S. Avramov et al., Automatic inductance voltage divider bridge for operation from 10 Hz to 100 kHz, *IEEE Trans. Instrum. Meas.,* **42**: 131–135, 1993.
26. R. Yell, NPL MK 3 WBCO attenuator, *IEEE Trans. Instrum. Meas.,* **IM-27**: 388–391, 1978.
27. R. Yell, Developments in waveguide below cutoff attenuators at NPL, *IEE Colloquim Dig.,* **49**: 1/1–1/5, 1981.
28. H. Bayer, Consideration of a rectangular waveguide below cutoff piston attenuator as a calculable broad-band attenuation standard between 1 MHz and 2.6 GHz, *IEEE Trans. Instrum. Meas.,* **IM-29**: 467–471, 1980.
29. F. L. Warner, D. O. Watton, and P. Herman, A very accurate X-band rotary vane attenuator with an absolute digital angular measurement system, *IEEE Trans. Instrum. Meas.,* **IM-21**: 446–450, 1972.
30. W. E. Little, W. Larson, and B. J. Kinder, Rotary vane attenuator with an optical readout, *J. Res. NBS,* **75C**: 1–5, 1971.
31. W. Larson, *The Rotary Vane Attenuator as an Interlaboratory Standard,* NBS Monograph 144, Washington, DC: US Government Printing Office, November 1975.
32. H. Bayer, F. Warner, and R. Yell, Attenuation and ratio-national standards, *Proc. IEEE,* **74**: 46–59, 1986.
33. T. Imamura, MN9002 Standard optical attenuator, *Annitsu Techn. Rev.,* **14**: 32–41, 1991.
34. G. F. Engen and R. W. Beatty, Microwave attenuation measurements with accuracies from 0.0001 to 0.06 dB over a range of 0.01 to 50 dB, *J. Res. NBS,* **64C**, 139–145, 1960.
35. H. Bayer, An error analysis for the RF-attenuation measuring equipment of the PTB applying the power method, *Metrologia,* **11**: 43–51, 1975.
36. D. L. Hollway and F. P. Kelly, A standard attenuator and the precise measurement of attenuation, *IEEE Trans. Instrum. Meas.,* **IM-13**: 33–44, 1964.
37. F. L. Warner, P. Herman, and P. Cumming, Recent improvements to the UK national microwave attenuation standards, *IEEE Trans. Instrum. Meas.,* **IM-32** (1): 33–37, 1983.
38. F. K. Weinert, High performance microwave ratio meter employs paralle if complex vector substitution, *Microw. J.,* **24**: 51–85, 1981.
39. Hewlett-Packard, *Understanding the Fundamental Principles of Vector Network Analysis,* HP Application Note 1287-1, 1997; *Exploring the Architectures of Network Analyzers,* HP Application Note 1287-2, 1997; *Applying Error Correction to Network Analyzer Measurement,* HP Application Note 1287-3, 1997.
40. G. F. Engen, Microwave circuit theory and foundations of microwave metrology, *IEE Electrical Measurement Series,* **9**, London: Perigrinus, 1992.
41. O. D. D. Soares (ed.), Trends in optical fibre metrology, *Part VI: Optical Fibre Characterisation, Calibration Standards,* Fibre Characterization and Measurement, p. 353–397; NATO ASI Series E, Applied Sciences, Dordrecht: Kluwer, 1995, Vol. 285.
42. C. Hentschel, *Fibre Optics Handbook,* Hewlett Packard, HP 13100-5952-9654, Boblingen, Germany: Hewlitt Packard, 1989.
43. International Electrotechnical Commission, Optical fibres-Part 1: Generic specification IEC 793-1 (11/92).
44. International Telecommunications Union, Definition and test methods for the relevant parameters of single mode fibres, ITU-T G 650 (03/93).
45. T. Jones, Attenuation and cut-off wavelength measurement, National Physical Laboratory, Optical Fibre Measurement Course, April 27–28, 1993.
46. D. J. Ives and B. Walker, Optical time domain reflectometry, National Physical Laboratory, Optical Fibre Measurement Course, April 27–28, 1993.

47. International Organization for Standardization, Guide to the expression of uncertainty in measurement, 1st ed., Geneva, Switzerland: International Organization for Standardization, ISBN 92-67-10188-9. 1993, corrected and reprinted 1995.
48. European Cooperation for Accreditation of Laboratories, *Expression of the Uncertainty of Measurement in Calibration,* EAL-R2, Edition 1, April 1997; *Examples,* EAL-R2-S1, Edition 1, November 1997.
49. I. A. Harris and F. L. Warner, Re-examination of mismatch uncertainty when measuring microwave power and attenuation, *IEE Proc., Pt. H,* **128** (1): 35–41, 1981.

KURT HILTY
Swiss Federal Office of Metrology

ATTENUATION MEASUREMENTS. See ACOUSTIC WAVE INTERFEROMETERS.